Article

Cell

Astrocytic Insulin Signaling Couples Brain Glucose Uptake with Nutrient Availability

Graphical Abstract

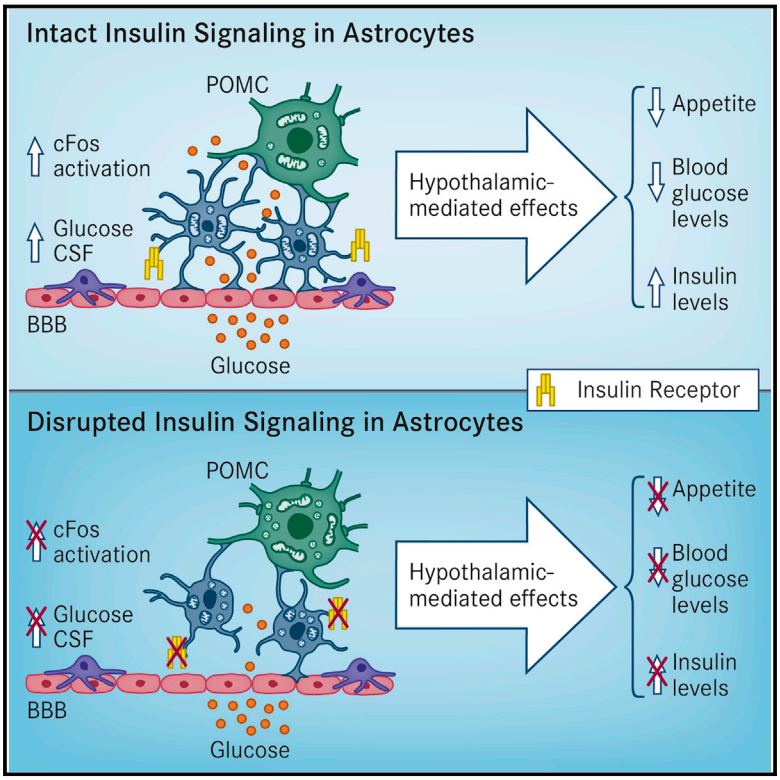

Highlights

- Astrocytic IRs control glucose-induced activation of hypothalamic POMC neurons
- Hypothalamic IRs in astrocytes regulate CNS and systemic glucose metabolism
- Astrocytic IRs are required for proper glucose and insulin entry to the brain

Authors

Cristina García-Cáceres, Carmelo Quarta, Luis Varela, ..., Magdalena Götz, Tamas L. Horvath, Matthias H. Tschöp

Correspondence

tschoep@helmholtz-muenchen.de

In Brief

Insulin sensing by hypothalamic astrocytes co-regulates brain glucose sensing and systemic glucose metabolism.

García-Cáceres et al., 2016, Cell *166*, 867–880
August 11, 2016
http://dx.doi.org/10.1016/j.cell.2016.07.028

CellPress

Cell

Astrocytic Insulin Signaling Couples Brain Glucose Uptake with Nutrient Availability

Cristina García-Cáceres,[1,2] Carmelo Quarta,[1,2] Luis Varela,[3] Yuanqing Gao,[1,2] Tim Gruber,[1,2] Beata Legutko,[1,2] Martin Jastroch,[1,2] Pia Johansson,[4,5,6] Jovica Ninkovic,[4,5,6] Chun-Xia Yi,[1,2] Ophelia Le Thuc,[1,2] Klara Szigeti-Buck,[3] Weikang Cai,[7] Carola W. Meyer,[1,2] Paul T. Pfluger,[1,2] Ana M. Fernandez,[8] Serge Luquet,[9] Stephen C. Woods,[10] Ignacio Torres-Alemán,[8] C. Ronald Kahn,[7] Magdalena Götz,[4,5,6] Tamas L. Horvath,[3] and Matthias H. Tschöp[1,2,*]

[1]Helmholtz Diabetes Center (HDC) & German Center for Diabetes Research (DZD), Helmholtz Zentrum München, 85764 Neuherberg, Germany

[2]Division of Metabolic Diseases, Technische Universität München, 80333 Munich, Germany

[3]Program in Integrative Cell Signaling and Neurobiology of Metabolism, Section of Comparative Medicine, Yale University School of Medicine, New Haven, CT 06520, USA

[4]Institute of Stem Cell Research Center, Helmholtz Zentrum München, 85764 Neuherberg, Germany

[5]Physiological Genomics, Biomedical Center, Ludwigs-Maximilians-University, 80336 Munich, Germany

[6]7SYNERGY, Excellence Cluster Systems Neurology, Biomedical Center, Ludwigs-Maximilians-University, 80336 Munich, Germany

[7]Section of Integrative Physiology and Metabolism, Joslin Diabetes Center and Department of Medicine, Brigham and Women's Hospital and Harvard Medical School, Boston, MA 02115, USA

[8]Institute Cajal, CSIC, 28002 Madrid, Spain

[9]Université Paris Diderot, Sorbonne Paris Cité, Unité de Biologie Fonctionnelle et Adaptative, CNRS UMR 8251, 75205 Paris, France

[10]Department of Psychiatry and Behavioral Neuroscience, University of Cincinnati, 2170 Galbraith Avenue, Cincinnati, OH 45237, USA

*Correspondence: tschoep@helmholtz-muenchen.de

http://dx.doi.org/10.1016/j.cell.2016.07.028

SUMMARY

We report that astrocytic insulin signaling co-regulates hypothalamic glucose sensing and systemic glucose metabolism. Postnatal ablation of insulin receptors (IRs) in glial fibrillary acidic protein (GFAP)-expressing cells affects hypothalamic astrocyte morphology, mitochondrial function, and circuit connectivity. Accordingly, astrocytic IR ablation reduces glucose-induced activation of hypothalamic pro-opio-melanocortin (POMC) neurons and impairs physiological responses to changes in glucose availability. Hypothalamus-specific knockout of astrocytic IRs, as well as postnatal ablation by targeting glutamate aspartate transporter (GLAST)-expressing cells, replicates such alterations. A normal response to altering directly CNS glucose levels in mice lacking astrocytic IRs indicates a role in glucose transport across the blood-brain barrier (BBB). This was confirmed in vivo in GFAP-IR KO mice by using positron emission tomography and glucose monitoring in cerebral spinal fluid. We conclude that insulin signaling in hypothalamic astrocytes co-controls CNS glucose sensing and systemic glucose metabolism via regulation of glucose uptake across the BBB.

INTRODUCTION

Glucose availability in the CNS is critical for neuronal function, and glucose levels in the brain regulate local neuronal activity and whole-body energy metabolism. Although glucose handling in the brain has been considered an insulin-independent process (Cranston et al., 1998; Hasselbalch et al., 1999), an open debate exists about the role of insulin action in controlling cerebral glucose metabolism. Several lines of evidence suggest that insulin signaling regulates central and systemic metabolic homeostasis (Brüning et al., 2000; Woods et al., 1979). However, the molecular mechanisms and the main cellular targets mediating central actions of insulin are far from being completely understood.

Interestingly, alterations in the insulin-CNS axis have been associated with the progression of some neurodegenerative diseases, including Alzheimer's disease (Kleinridders et al., 2014; Koch et al., 2008), indicating that an inappropriate control of central insulin signaling might be relevant for pathological conditions affecting neuronal integrity and function. Insulin receptors (IRs) are widely distributed in the CNS (Havrankova et al., 1978) and abundantly expressed in epithelial cells in the choroid plexus and in brain endothelial cells (Frank et al., 1986). Cerebral blood vessels are ensheathed by endothelial cells that interact with adjacent astrocytes, the combination regulating the entry of nutrients, such as glucose, by changes in blood-brain barrier (BBB) permeability (Alvarez et al., 2013). Importantly, regulation of blood glucose supply to and within the brain is controlled via glucose transporter (GLUT)-1 (Abbott et al., 2006; Armulik et al., 2010). Although GLUT-1 is highly expressed along the BBB in both endothelial cells and astrocytes (Barros et al., 2007; Simpson et al., 2001), it is more abundant in astrocytes (Simpson et al., 1999). Astrocytes are the most abundant cells in the brain, and they provide a nurturing environment regulating all aspects of neuronal function, including synaptic plasticity, survival, development, metabolism, and neurotransmission, among others. In fact, astrocytes are able to respond to local levels of nutrients, acting as metabolic sensors and expressing specific receptors and transporters extending throughout their membrane surface (García-Cáceres et al., 2012). Consistent with this, astrocytes are located at the interface

Table 1. Specificity and Efficiency of Inducible Cre-Mediated Recombination in Adult Mice Heterozygous for GLAST^{CreERT}:tdTomato/eGFP Treated with Tamoxifen

Specificity (%/Section)	Hypothalamus (%)
% GFAP/GFP	61.8 ± 6.5 (n = 11)
% S100β/GFP	45.7 ± 2.4 (n = 9)
Efficiency (%/Section)	**Hypothalamus (%)**
% GFP/GFAP	27.0 ± 8.5 (n = 11)
% GFP/S100β	54.9 ± 3.3 (n = 21)

between vessels and neurons, putting them in a privileged position to control glucose fluxes between the periphery and the CNS. However, the possibility that insulin signaling in astrocytes plays a functional role in systemic metabolism has never been studied. We therefore used a series of glia-specific loss-of-function models to uncover the function of astrocytic insulin signaling in the brain and, more specifically, for hypothalamic glucose sensing.

RESULTS

Postnatal Ablation of Insulin Receptors from Astrocytes

To uncover the role of IRs in astrocytes, we used a Cre/lox approach to genetically remove IRs exclusively from human glial fibrillary acidic protein (hGFAP)- and glutamate aspartate transporter (GLAST)-positive cells. Because glial cells act as neuronal progenitor cells during brain development (Goldman, 2003), we generated tamoxifen-inducible transgenic hGFAP-CreER^{T2} (Ganat et al., 2006) and knockin GLAST^{CreERT2} (Buffo et al., 2008; Mori et al., 2006) mouse models to achieve time-specific IR flox/flox ($^{f/f}$) deletion in adult mice. Using Rosa26 ACTB-tdTomato/EGFP (tdTomato/eGFP) reporter mice, we confirmed that Cre-mediated recombination occurred following intraperitoneal (i.p.) tamoxifen (Tx) injection (Figure S1A). In agreement with previous studies demonstrating that both hGFAPCreER^{T2} (Kim et al., 2014) and GLAST^{CreERT2} (Mori et al., 2006) mouse models are suitable to achieve Cre-mediated recombination in astrocytes, we observed that virtually all of the Cre-recombined cells in the mediobasal hypothalamus (MBH) exhibited the stellated morphology characteristic of astrocytes, as well as immunoreactivity for GFAP and S100β after Tx administration (Figure S1B; Table 1). To demonstrate IR deletion in cells undergoing Cre-recombination, we crossed hGFAP-CreER^{T2}:IR$^{f/f}$ and IR$^{f/f}$ mice with hGFAP-eGFP mice in which the fluorescent protein GFP was placed under control of the human GFAP promoter (Nolte et al., 2001). Using this reporter mouse model, we purified hGFAP-GFP+ cells from brains of adult mice by fluorescence-activated cell sorting (FACS) and confirmed that IR expression was significantly reduced exclusively in the brains of hGFAP-CreER^{T2}:IR$^{f/f}$ mice treated with Tx (named GFAP-IR KO mice; Figure 1A). IR mRNA expression was absent from GFP-targeted astrocytes in the hypothalamus of GLAST-IR KO mice (GLAST^{CreERT2}:IR$^{f/f}$ mice injected with Tx) and crossed with tdTomato/eGFP mice, whereas IR mRNA was present in astrocytes of GLAST-IR wild-type (WT) mice (Figures 1B and S1C).

Finally, we confirmed that insulin treatment enhanced protein kinase B (Akt) activation in hypothalamic GFAP-positive cells of GFAP-IR WT mice (IR$^{f/f}$ mice treated with Tx), but not in GFAP-IR KO mice (Figure 1C). In contrast, similar levels of Akt activation were observed in peripheral insulin-sensitive tissues (e.g., liver, skeletal muscle, and adipose tissue) of mice with or without IRs in astrocytes (Figure S2), demonstrating that the loss of IRs in astrocytes uniquely reduced insulin signaling activation in astrocytes of the brain.

Insulin Receptors Control Glucose Availability in Astrocytes

Next, we assessed the impact of IR ablation on glucose availability in astrocyte cultures from the hypothalamus of IR$^{f/f}$ male pups at postnatal day 1 in which IR deletion was induced by adenovirus Cre-mediated recombination. First, we confirmed that adenoviral-based vectors mediated Cre-recombination widely in astrocyte cultures, succeeding in reducing IRβ protein levels (Figure 1D), IR expression levels (Figure 1E), and the ability of astrocytes to phosphorylate Akt following insulin administration (Figures 1F and 1G). Moreover, the loss of IRs in astrocytes resulted in a lower glucose uptake upon stimulation with glucose (Figure 1H), consistent with a reduced glycolytic rate (Figure 1I), lower GLUT-1 expression levels (WT: 1.00 ± 0.09, n = 6 versus KO: 0.63% ± 0.09% of WT values, n = 6; $p < 0.02$) and decreased L-lactate efflux (Figure 1J) in those glial cells. However, no differences were observed in cellular glycogen content among experimental groups (Figure 1K). Despite having a lower glycolytic flux, astrocytes without IRs exhibited higher basal mitochondrial respiration (Figure 1L), and this was associated with higher expression levels of carnitine palmitoyltransferase 1C (CPT1C), the key enzyme responsible for long-chain fatty acid transport into mitochondria (Figure 1M). To corroborate that the lack of IRs in astrocytes elevated mitochondrial fatty acid (beta)-oxidation for compensation of reduced glucose uptake, we used etomoxir to inhibit CPT1C and thus fatty acid oxidation. Indeed, etomoxir reduced basal mitochondrial respiration (Figure 1N) and maximal substrate oxidation (Figure 1O), without causing changes in glycolytic rate (Figure S3A).

Next, we examined whether insulin signaling in astrocytes controls mitochondrial responses to glucose. We found that hypothalamic astrocytes of GFAP-IR WT mice responded to elevated systemic glucose levels by reducing the overall mitochondrial area, whereas there was no such significant change in hypothalamic astrocytes of GFAP-IR KO mice (Figure S3B). Despite having no reduced cytosolic mitochondria area, astrocytes from the hypothalamus of GFAP-IR KO mice did have a reduced mitochondrial aspect ratio, a parameter reflecting mitochondrial length, due to fewer elongated mitochondria (asterisks; Figures 2A and 2B), and an increase in the presence of autophagosomes (arrows; Figures 2C and 2D) in response to elevated blood glucose. Both parameters remained unchanged in GFAP-IR WT mice.

Astrocyte-Specific Loss of Insulin Receptors Affects Astroglial Morphology

To verify a morphological impact following loss of astrocytic IRs in vivo, and given the effect of insulin-related peptides on astroglial differentiation (Toran-Allerand et al., 1991), we analyzed whether the morphology of hypothalamic astrocytes

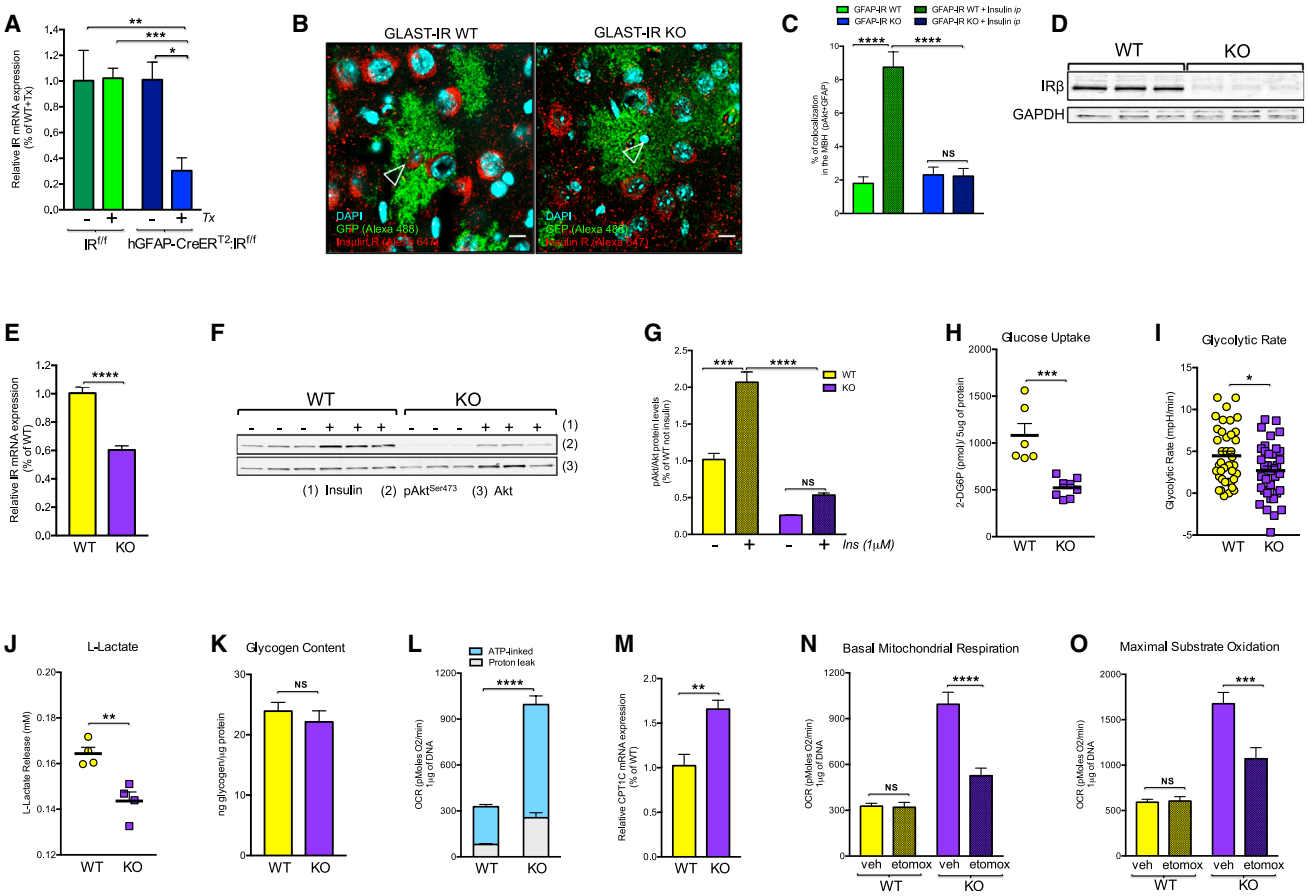

Figure 1. In Vivo and Ex Vivo Ablation of Astrocytic IRs Reduces Insulin Signaling and Glucose Availability in Astrocytes

(A) Insulin receptor (IR) mRNA expression levels in purified GFAP-positive cells from brains of adult IR flox/flox ($^{f/f}$) mice or hGFAP-CreER^{T2}:IR$^{f/f}$ mice after administration with (+) or without (–) tamoxifen (Tx) injection (n = 3–10/group).

(B) In situ hybridization combined with immunofluorescence for the visualization of IR mRNA (empty arrows; red, Alexa 647) in the GFP-expressing astrocytes under the promoter of GLAST (green fluorescence) from hypothalamic sections of GLAST-IR WT mice and GLAST-IR KO mice crossed with tdTomato/eGFP reporter mice (see also Figure S1; Table 1).

(C) Percentage of positive colocalization of pAkt and GFAP-positive cells quantified in the hypothalamus of GFAP-IR WT mice and GFAP-IR KO mice 15 min after vehicle (saline) or insulin injection (i.p.; 3 IU/kg bw) (n = 4 mice/group) (see also Figure S2 for peripheral tissue).

(D) Protein levels of IRβ and GAPDH in primary hypothalamic astrocytes of IR$^{f/f}$ male mice treated with adenovirus-driven GFP expression (WT; n = 3) or driven Cre recombinase with GFP expression (KO; n = 3).

(E) IR mRNA expression levels in primary hypothalamic astrocytes with (WT) or without (KO) IRs (n = 6/ group).

(F and G) Western blots (F) and quantification (G) of the ratio between phosphorylated Akt in serine 473 (pAkt^{Ser473}) and total Akt protein levels in primary hypothalamic astrocytes with (WT) or without (KO) IRs 5 min after vehicle or insulin stimulation (1 μM; n = 3/group).

(H–K) Cellular accumulation of 2-DG6P (in pmol/5 μg of protein; n = 6–8/group) (H), glycolytic rate (n = 35 replicates/group from four different experimental cultures) (I), L-Lactate production levels in medium (in mM; n = 4/group) (J), and glycogen content (ng of glycogen/μg of protein; n = 4/group) in primary hypothalamic astrocytes with (WT) or without (KO) IRs (K).

(L and M) Basal mitochondrial respiration (OCR; pmo of oxygen/min per 1 μg of DNA: n = 35 replicates/group from four different experimental cultures) (L) and CPT1C expression levels (n = 4/group) in primary hypothalamic astrocytes with (WT) or without (KO) IRs (M).

(N and O) Etomoxir effect on basal mitochondrial respiration (OCR) (N) or maximal substrate oxidation (pmol of oxygen/min per 1 μg of DNA) (O) in hypothalamic astrocytes with (WT) or without (KO) IRs treated with vehicle (veh) or etomoxir (etomox: 40 μm) (n = 12–36 replicates/4 different experimental cultures) (see also Figure S3A).

Akt, protein kinase B; CPT1C, carnitine palmitoyltransferase 1C; GAPDH, glyceraldehyde-3-phosphate dehydrogenase; GFAP, glial fibrillary acidic protein; GLAST, glutamate aspartate transporter; IR, insulin receptor; OCR, oxygen consumption rate; pAkt, phosphorylation in Serine 473 of Akt; Tx, tamoxifen. ****p < 0.0001; ***p < 0.001; **p < 0.01; *p < 0.05. NS, no significant differences between groups. Data are presented as the mean ± SEM. Scale bars, 100 μm.

was affected following loss of IRs in vivo. While postnatal astrocyte-specific loss of IRs did not alter the total number of hypothalamic GFAP-positive cells (GFAP-IR WT: 93.7 ± 4.4: n = 39 versus GFAP-IRKO: 80.7 ± 5.6: n = 39 astrocyte number /field), fewer (Figure 2E) and shorter (Figure 2F) primary astrocyte processes were quantified in GFAP-IR KO mice compared to levels in GFAP-IR WT mice (Figure 2G), indicating a potentially altered interaction with surrounding cells. A comparable reduction in the

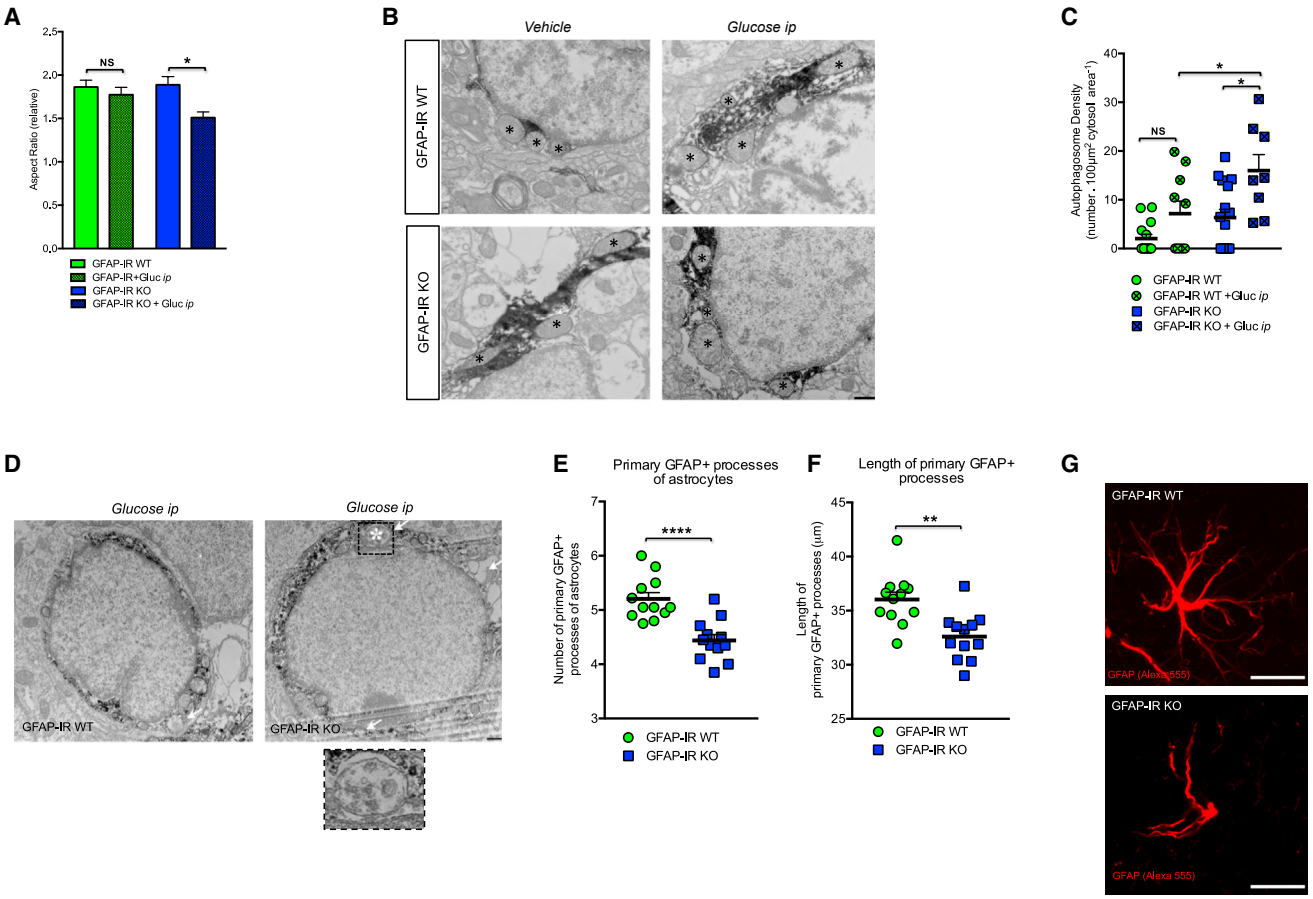

Figure 2. Astrocytic Insulin Signaling Regulates Mitochondria Network and Structural Changes in Hypothalamic Astrocytes

(A and B) Quantification of (A) and electron microscopic images depicting (B) the mitochondrial aspect ratio (asterisks → mitochondria) in astrocytes from the hypothalamus of GFAP-IR WT mice and GFAP-IR KO mice 30 min after i.p. glucose injection (n = 3–4 brains per group) (see also Figure S3B).

(C and D) Quantification of (C) and electron microscopic images depicting (D) mitochondrial autophagosome density (arrow → autophagosome) in astrocytes from the hypothalamus of GFAP-IR WT mice and GFAP-IR KO mice 30 min after i.p. glucose injection (n = 3–4 brains per group).

(E and F) Quantification of the number of primary projections (E) and the length of their astrocyte processes (F) in the hypothalamus of GFAP-IR WT versus GFAP-IR KO mice (n = 20 brain sections/group) (see also Figures S3C and S3D for the hippocampus).

(G) High-magnification image depicting the morphological differences between GFAP-positive cells (red, Alexa 555) from the hypothalamus of GFAP-IR WT mice versus those from GFAP-IR KO mice.

GFAP, glial fibrillary acidic protein; IR, insulin receptor. ****$p < 0.0001$; **$p < 0.01$; *$p < 0.05$. NS, no significant differences between groups. Data are presented as the mean ± SEM. Scale bars, 500 nm (B and D) and 10 μm (G).

number of primary projections was also seen in extra-hypothalamic areas, such as the hippocampus (Figure S3C), whereas no changes were detected in the length of the astrocyte processes in this area (Figure S3D).

Astrocyte-Specific Loss of Insulin Receptors Reduces Glucose Sensing in Specific Hypothalamic Brain Nuclei and Pro-opio-melanocortin Neurons

To evaluate glucose sensing in the hypothalamus in response to systemic glucose fluctuations, we examined c-Fos immunoreactivity in specific hypothalamic areas following intraperitoneal (i.p.) glucose injection. GFAP-IR KO mice had a reduced number of glucose-induced, activated (c-Fos) cells in the dorsomedial hypothalamus (DMH) (Figures 3A and 3B). No significant differences were observed in response to elevated blood glucose levels in the number of c-Fos immunoreactive cells in other hypothalamic areas analyzed, including the ventromedial hypothalamus (VMH), lateral hypothalamus (LH), and the arcuate nucleus of the hypothalamus (ARC) (Figure 3B). Even though peripheral glucose injection increased the total number of c-Fos-labeled cells in the ARC of both groups, mice lacking astrocytic IRs had less of an increase in the number of glucose-activated pro-opio-melanocortin (POMC) neurons (c-Fos-immunoreactive) in response to i.p. glucose (Figures 3C and 3D).

Astrocyte-Specific Loss of Insulin Receptors Affects Mitochondrial Integrity and Mitochondria-ER Contacts in POMC Neurons

Cellular adaptations to fluctuations in nutrient availability involve the regulation of mitochondrial function, a process intimately

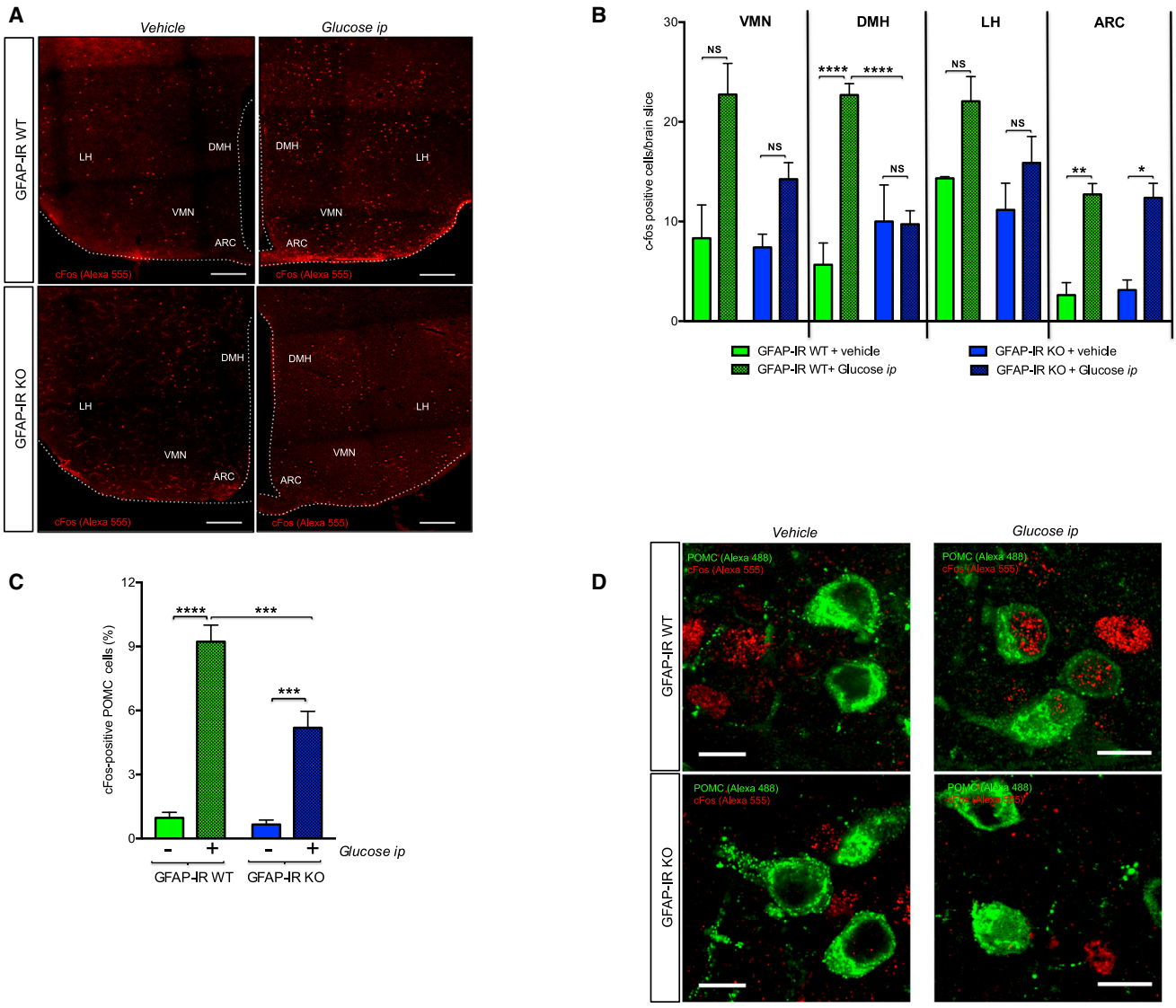

Figure 3. Insulin Receptors in Astrocytes Control Glucose-Induced c-Fos Activation in Hypothalamic POMC Neurons

(A) Brain sections depicting c-Fos immunoreactive cells (red, Alexa 555) in specific glucose-sensing hypothalamic nuclei of GFAP-IR WT mice and GFAP-IR KO mice 2 hr after vehicle or i.p. glucose injection.

(B) The number of c-Fos immunoreactive cells found in the ventromedial hypothalamus (VMN), dorsomedial hypothalamus (DMH), lateral hypothalamus (LH), and arcuate nucleus of the hypothalamus (ARC) of GFAP-IR WT mice and GFAP-IR KO mice 2 hr after vehicle or i.p. glucose (n = 3–4 brains/group).

(C) Analysis of c-Fos immunoreactivity in POMC neurons 2 hr after vehicle or i.p. glucose injection in GFAP-IR WT mice versus GFAP-IR KO mice (n = 3–4 mice/group). Data are expressed as percentage of total POMC cells having c-Fos immunoreactivity per section.

(D) Images depicting POMC (green; Alexa 488) and c-Fos (red; Alexa 555)-positive cells in GFAP-IR WT mice versus GFAP-IR KO mice 2 hr after vehicle or i.p. glucose injection.

ARC, the arcuate nucleus of the hypothalamus; DMN, the dorsomedial hypothalamus; GFAP, glial fibrillary acidic protein; IR, insulin receptor; LH, the lateral hypothalamus; POMC, pro-opio-melanocortin; VMN, the ventromedial hypothalamus. p values = ****p < 0.0001; ***p < 0.001; **p < 0.01; *p < 0.05. NS, no significant differences between groups. Scale bars, 200 μm (A) and 10 μm (D).

associated with changes in neuron-mitochondrial network complexity (Baltzer et al., 2010; Mandl et al., 2009). Indeed, we found that POMC neurons of mice lacking IRs in astrocytes had reduced mitochondrial density (Figure S3E) and mitochondrial coverage (Figure S3F) in response to high peripheral glucose levels, whereas no differences were found in GFAP-IR WT mice. Both groups had an elevated mitochondrial aspect ratio in POMC neurons in response to i.p. glucose injection (Figure S3G). GFAP-IR KO mice had an increase in the number of autophagosomes (asterisks; Figures 4A and 4B) and disrupted mitochondria (arrows; mitochondria in autophagic processes) in the cytosol of POMC neurons (Figures 4C and 4D).

Finally, we examined the number of ER-mitochondrial contacts of POMC neurons, contacts essential for structural

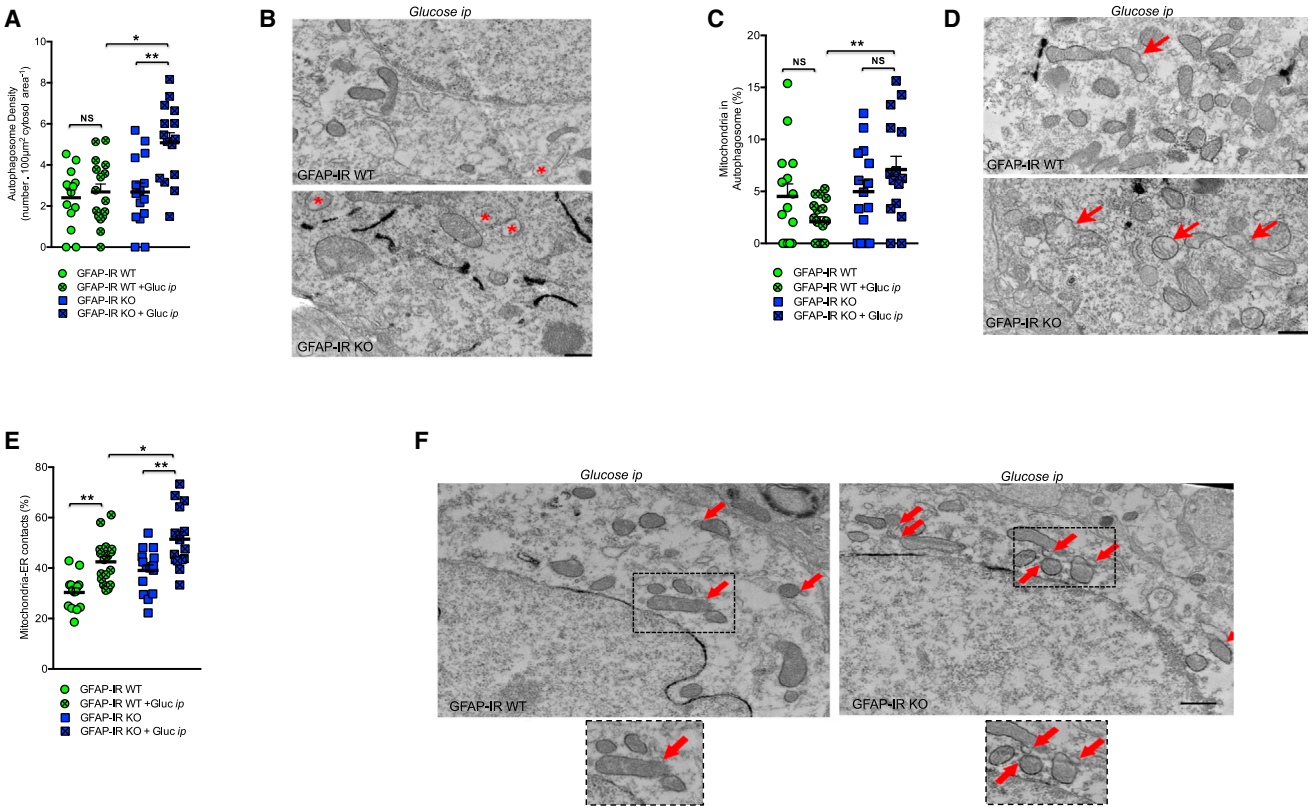

Figure 4. Postnatal Ablation of Astrocytic IRs Alters Mitochondria-ER Network Adaptations to Glucose in POMC Neurons

(A and B) Quantification of (A) and electron microscopic images depicting (B) autophagosomes (asterisk→ autophagosome) in POMC neurons of GFAP-IR WT mice and/or GFAP-IR KO mice (n = 14–16 measurements from 3–4 mice/group).

(C and D) Quantification of (C) and electron microscopic images depicting (D) mitochondria in autophagosomes (arrow→ disrupted mitochondrion or loss of mitochondrial membrane integrity) in POMC neurons of GFAP-IR WT mice and/or GFAP-IR KO mice (n = 14–16 measurements from 3–4 mice/group) (see also Figures S3E–S3G).

(E and F) Quantification of (E) and electron microscopic images (F) depicting mitochondria-ER contacts (arrow→ mitochondrion in direct contact with ER processes) in the cytosol of POMC neurons of GFAP-IR WT mice and/or GFAP-IR KO mice (n = 14–16 measurements from 3–4 mice/group).

GFAP, glial fibrillary acidic protein; ER, endoplasmic reticulum; IR, insulin receptor; POMC, pro-opio-melanocortin. **p < 0.01; *p < 0.05. NS, no significant differences between groups. Data are presented as the mean ± SEM. Scale bars, 500 nm.

support and functional interorganellar communication regulating Ca^{2+} homeostasis, metabolism of glucose, phospholipids, and cholesterol (Tubbs et al., 2014). After peripheral glucose administration, GFAP-IR KO mice had higher number of ER-mitochondrial contacts in POMC neurons relative to GFAP-IR WT mice (arrows; Figures 4E and 4F). Taken together, these findings suggest that the lack of IRs in astrocytes induces alterations in neural-mitochondrial network responses to glucose, which may impair POMC neurons to appropriately respond to cellular metabolic needs.

Astrocyte-Specific Loss of Insulin Receptors Alters Glial Coverage Remodeling and Synaptic Input Organization on Hypothalamic POMC Neurons

To evaluate whether our observed changes in astrocyte morphology and c-Fos activation affect hypothalamic neural circuits controlling systemic glucose homeostasis, we analyzed the patterns of glial ensheathment of perikaryal membranes of immunoreactive POMC neurons in the hypothalamus. Mice lacking IRs exclusively in astrocytes responded to peripheral glucose injection by less glial coverage of POMC neurons than occurred in control mice (Figure 5A), as indicated by using electron (Figure 5B) or confocal microscopy (Figure 5C; GFAP-IR WT + glucose i.p.: 26.81 ± 2.2; n = 15 versus GFAP-IR KO + glucose i.p.: 11.8% ± 1.9% of astrocyte coverage per POMC cell; n = 12; p < 0.002). Finally, we analyzed the impact of glial coverage changes on the number and type of synaptic profiles on POMC neurons. There was an increase in the number of symmetric synapses (Figure S3H) and no change in the number of asymmetric synapses (Figure S3I) in response to peripheral glucose injection in both groups. However, the overall changes in the synaptic profile of POMC neurons in GFAP-IR KO mice resulted in an elevated number of total synapses on POMC perikarya (Figures 5D and 5E).

Astrocytic Insulin Signaling Controls Systemic Glucose Homeostasis

To determine whether astrocyte-specific IRs are involved in maintaining glucose homeostasis, we examined dynamic

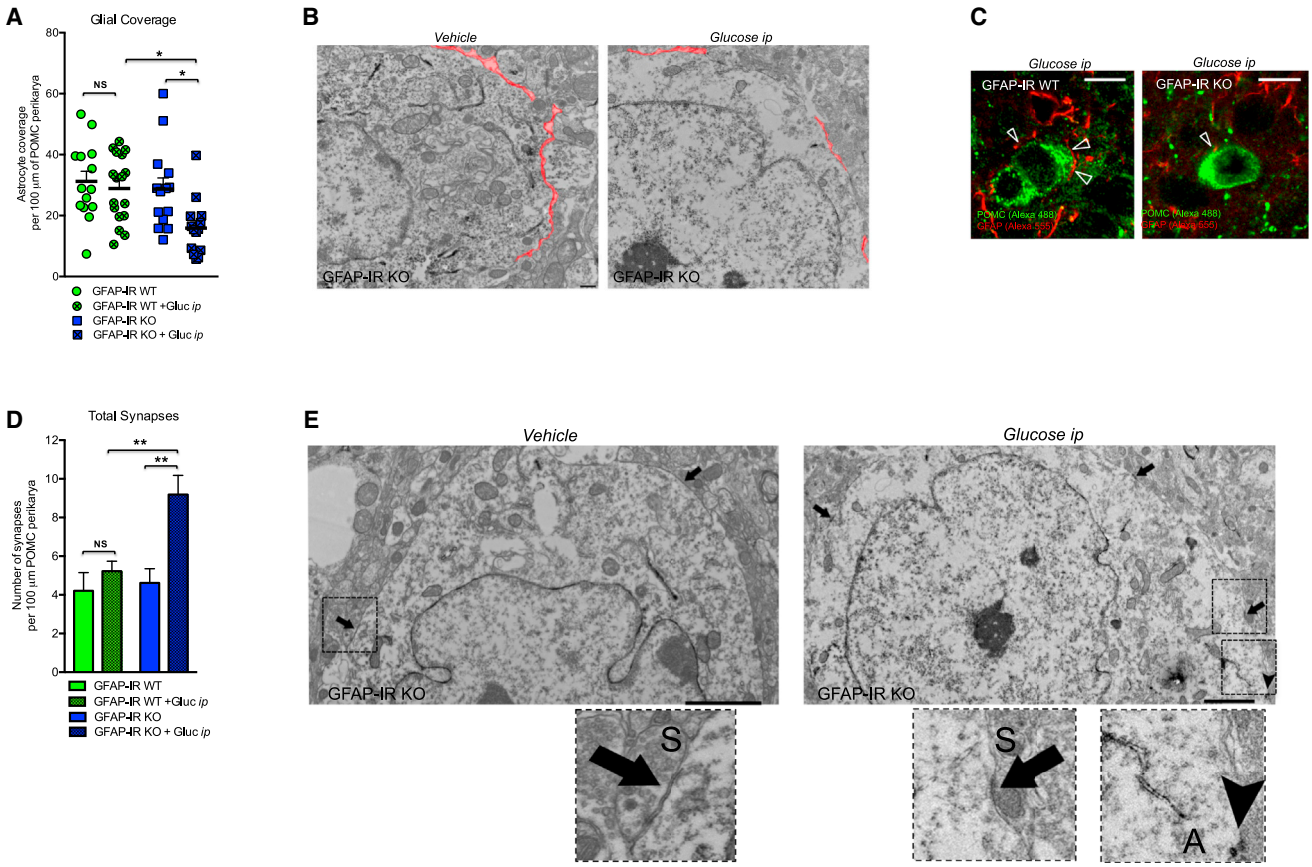

Figure 5. Insulin Signaling in Astrocytes Regulates Glial Coverage and Synaptic Profile of POMC Neurons in Response to Elevated Systemic Glucose Levels

(A and B) Quantification of (A) and electron microscopic images depicting (B) glial coverage of the membrane of hypothalamic POMC neurons of GFAP-IR WT mice and/or GFAP-IR KO mice 30 min after vehicle or i.p. glucose injection (n = 3–4 mice/group).

(C) Hypothalamic images depicting GFAP-labeled processes (red, Alexa 555) in direct contact (arrows) with the membrane of POMC neurons (green, Alexa 488) in the hypothalamus of GFAP-IR WT mice versus GFAP-IR KO mice 30 min after i.p. glucose injection.

(D and E) Quantification of (D) and electron microscopic images depicting (E) the total number of synapses for the membrane of hypothalamic POMC neurons of GFAP-IR WT mice and/or GFAP-IR KO mice 30 min after vehicle or i.p. glucose injection (n = 3–4 mice/group). Symmetric synapses (S) → arrows. Asymmetric synapses (A) → head-arrow (for synapses quantifications, see Figures S3H and S3I).

GFAP, glial fibrillary acidic protein; IR, insulin receptor; POMC, pro-opio-melanocortin. $^{**}p < 0.01$; $^{*}p < 0.05$. NS, no significant differences between groups. Data are presented as the mean ± SEM. Scale bars, 500 nm (B), 10 µm (C), and 2 µm (E).

feeding behavior and glucose regulatory responses to altered systemic glucose availability. First, mice with or without astrocytic IRs were subjected to a fasting-induced hyperphagia paradigm to generate a physiological situation of reduced glucose availability. GFAP-IR KO mice were unable to appropriately curb the hyperphagic response to fasting, likely due to insufficient availability or delayed appearance of glucose in the brain (Figure 6A). Consistent with that possibility, GFAP-IR KO mice had a reduced suppression of fasting-induced hyperphagia in response to the administration of peripheral glucose (Figure 6B), a finding which may reflect reduced activation of POMC neurons. We also observed that GFAP-IR KO mice failed to efficiently readjust systemic glucose levels when subjected to hyperglycemia induced by peripheral glucose injection (Figure 6C). This effect was associated with a delayed response to increased peripheral insulin levels (Figure 6D). Consistent with that, those mice exhibited a higher area under the curve (AUC) of blood glucose levels in response to peripheral insulin injection (Figure 6E).

Next, we evaluated feeding in response to a peripheral glucose deficiency elicited by the glucoprivic agent, 2-deoxy-D-glucose (2DG) (Smith and Epstein, 1969). The expected physiological hyperphagic response was absent in mice lacking astrocytic insulin signaling (Figure 6F), demonstrating that astrocyte-specific loss of IRs impacts in vivo glucose metabolism.

GFAP-positive astrocytes only represent one subpopulation of astrocytes in the brain. We assessed whether the functional role of astrocytic insulin signaling in regulating glucose metabolism is restricted to the GFAP astrocyte-specific population or is also relevant for other astroglial populations such as

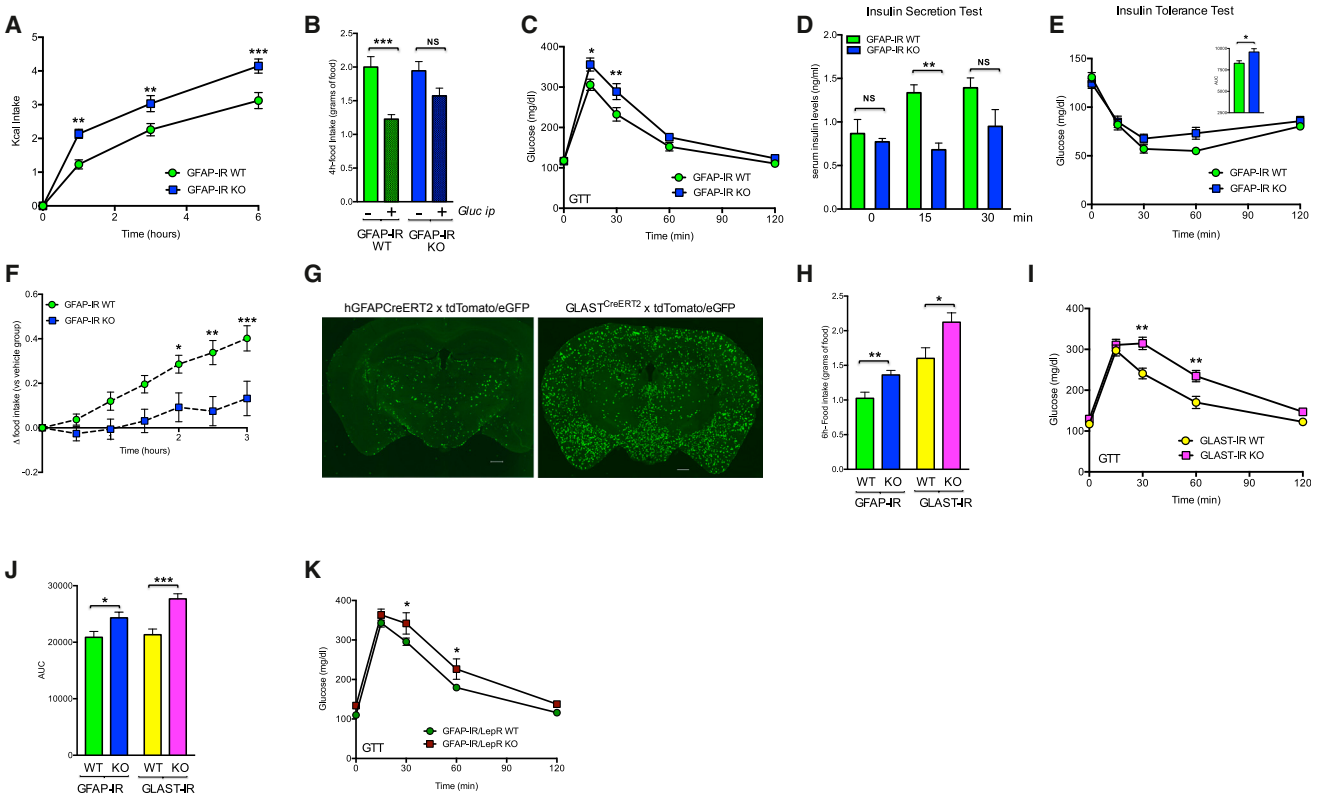

Figure 6. Insulin Receptors in GFAP and GLAST-Expressing Astrocytes Control CNS Glucose Sensing and Systemic Glucose Metabolism

(A) Food intake (kcal) in response to fasting in GFAP-IR WT mice and GFAP-IR KO mice (n = 8/group).

(B) 4 hr accumulated food intake in GFAP-IR WT mice and GFAP-IR KO mice after fasting and i.p. injection with vehicle or glucose (n = 8/group).

(C and D) Blood glucose (C) and serum insulin (D) levels in GFAP-IR WT mice and GFAP-IR KO mice after peripheral glucose injection (n = 8/group).

(E) Insulin tolerance test in GFAP-IR WT mice versus GFAP-IR KO mice (n = 8/group) after peripheral insulin injection.

(F) Increase in food intake elicited by i.p. 2-DG in GFAP-IR WT mice and GFAP-IR KO mice (n = 8/group).

(G) Images (coronal sections) of brains corresponding to hGFAP-CreER^{T2} mice or GLAST^{CreERT2} mice, which were crossed with tdTomato/eGFP mice after tamoxifen injection.

(H) 6 hr accumulated food intake in the refeeding phase between GLAST-IR WT mice and GLAST-IR KO mice (n = 5–8 mice/group) and between GFAP-IR WT mice and GFAP-IR KO mice (n = 10–12 mice/group).

(I) Blood glucose in GLAST-IR WT mice or GLAST-IR KO mice in response to i.p. glucose (n = 5–8 mice per group).

(J) Glucose tolerance test in GFAP-IR WT mice versus GFAP-IR KO mice (n = 10–12 mice per group) and GLAST-IR WT mice or GLAST-IR KO mice (n = 5–8 mice per group).

(K) Blood glucose levels of GFAP-IR/LepR WT mice (n = 12) versus GFAP-IR/LepR KO mice (n = 5) in response to i.p. glucose.

AUC, area under the curve; GFAP, glial fibrillary acidic protein; hGFAP, human glial fibrillary acidic protein; GLAST, glutamate aspartate transporter; GTT, glucose tolerance test; IR, insulin receptor; LepR, leptin receptor; 2DG: 2-deoxy-D-glucose. p values = ***p < 0.001; **p < 0.01; *p < 0.05. NS, no significant differences between groups. Data are presented as the mean ± SEM. Scale bars, 500 μm.

GLAST-expressing astrocytes. To accomplish that, we ablated IRs in astrocytes from adult GLAST^{CreERT2} mice (Figure 6G), and replicated the systemic glucose metabolic phenotype. GLAST-IR KO mice had an exaggerated fasting-induced hyperphagia comparable to that observed when we targeted IRs of GFAP-expressing cells (Figure 6H). In addition, those mice also had impaired regulation of systemic glucose levels in response to hyperglycemia (Figure 6I). Thus, both astrocyte-specific KO models had a significantly increased glucose AUC when compared to their respective WT groups (Figure 6J). Taken together, these findings confirm the relevance of a functional contribution of insulin signaling in astrocytes to systemic glucose control.

Mice Lacking Insulin Receptors in Astrocytes Exhibit a Systemic Glucose Metabolic Phenotype that Is Not a Direct Consequence of Mitochondrial Alterations in Hypothalamic Astrocytes

To evaluate whether the alterations in systemic glucose metabolism may simply be due to mitochondrial alterations in hypothalamic astrocytes of GFAP-IR KO mice, we generated a mouse model in which we altered astrocytic mitochondrial function by ablating uncoupling protein 2 (UCP2) in GFAP-positive cells of adult mice (named GFAP-UCP2 KO). Mice lacking UCP2 in astrocytes had a higher overall mitochondrial area in the cytosol of hypothalamic GFAP-positive cells (Figure S3J), and this was not associated with changes in their mitochondrial aspect ratio

(aspect ratio; Figures S3K and S3L). Despite mice having mitochondrial deregulation in astrocytes caused by the lack of UCP2, they did not exhibit altered glucose handling (Figure S3M), as we had observed in GFAP-IR KO mice. Thus, astrocytic mitochondrial changes per se, are unlikely cause of altered glucose control of astrocyte-specific IR conditional KO mice, but rather represent an adaptive consequence of altered glucose availability.

Integration of Energy-Related Signals in Astrocytes Contributes to Regulate Systemic Glucose Metabolism

Leptin and insulin are fundamental energy-related peripheral signals that have complementary yet distinct action in the brain. In order to dissect how both signals are integrated at the level of the astrocyte, we generated a specific adult double-knockout mouse model to simultaneously ablate both the insulin and leptin receptors (IR/LepR) in GFAP-positive cells of adult mice. Mice lacking both IR/LepR in astrocytes (hGFAP-CreER^{T2}- IR$^{f/f}$/LepR$^{f/f}$ treated with Tx) had a glucose intolerance phenotype compared to their control littermates (Figure 6K). These mice also exhibited elevated basal blood glucose levels (GFAP-IR/LepR WT mice: 109.8 ± 3.4; n = 12 versus GFAP-IR/LepR KO mice: 133.8 ± 6.8 mg/dl; n = 5; $p < 0.004$), thus not only showing replication but also enhancement of the glucose metabolic phenotype of astrocyte-specific IR knockout mice. These findings corroborate that hormone signaling in astrocytes has an important and previously underappreciated role in the control of systemic glucose metabolism.

Insulin Signaling in Hypothalamic Astrocytes Is Required for Systemic Glucose Homeostasis

Given that GFAP expression is also observed in non-CNS tissues (Sofroniew and Vinters, 2010) and that the hypothalamus plays a pivotal role in the central control of glucose homeostasis, we used a viral-mediated Cre/lox system approach to delete IRs exclusively in astrocytes located in the MBH. Using tdTomato/eGFP mice, we confirmed that viral delivery of Cre-recombination in hypothalamic GFAP-IR KO mice occurred specifically in astrocytes located in the infected area of the hypothalamus, which also exhibited immunoreactivity to both GFAP and S100β (Figures 7A and S3N; Table 2). Mice lacking IRs in hypothalamic astrocytes also had significantly decreased IR mRNA levels (Figure 7B) and failed to increase activation of Akt in MBH astrocytes in response to i.p. insulin injection (Figures 7C and 7D). Hypothalamic disruption of IRs in astrocytes of adult mice led to a phenotype that corresponded to that of GFAP-IR KO mice. Specifically, virus-assisted IR knockout in astrocytes of the MBH significantly impaired the systemic regulatory response to a peripheral glucose challenge (Figure 7E). Consistent with that observation, there was a reduction in 2DG-induced hyperphagia in those mice compared with littermate controls (Figures 7F–7H). These data collectively suggest that insulin signaling in hypothalamic astrocytes is required for efficient brain glucose handling.

Astrocytic Insulin Signaling Is Required for Adequate Insulin and Glucose Uptake into the Brain

To assess if astrocytic insulin signaling, in addition to being required for the CNS control of peripheral glucose homeostasis, also participates in the brain control of systemic energy balance, we compared the energy metabolic phenotype between GFAP-IR KO and GFAP-IR WT mice. No differences in body weight or weekly food intake were detected between groups on either standard chow or on a high-fat, high-sugar (HFHS) diet (Figure S3O). Next, we determined whether astrocytic insulin signaling may be directly required for CNS glucose availability. As a first step, we determined the impact of astroglial IR ablation on glucose uptake into the brain. Both GFAP-IR WT mice and GFAP-IR KO mice had comparably elevated systemic glucose levels after glucose challenge (Figure 7I). However, GFAP-IR KO mice failed to increase insulin levels in the cerebrospinal fluid (CSF), and a lower increase in CSF glucose was observed (Figures 7J and 7K). Accordingly, a lower glucose CSF/peripheral glucose ratio was found in mice lacking astrocytic insulin receptors exposed to elevated systemic glucose levels (Figure 7L). To corroborate these observations, we used in vivo ^{18}FDG positron emission tomography (PET) imaging to visualize and quantify glucose accumulation in the CNS. GFAP-IR KO mice had reduced brain glucose appearance in response to increased peripheral glucose levels (Figures 7M and 7N). Interestingly, the reduced brain glucose availability in GFAP-IR KO mice was associated with lowered brain expression of GLUT-1 (Figure 7O). Altogether, these data indicate key role for astrocytic insulin signaling in mediating proper glucose and insulin entry to the brain.

Astrocytic Insulin Signaling Is Expendable for Glucose Handling within the Brain

Astrocytes are well positioned to act as primary regulators of local CNS blood flow, nutrient flux, and synaptic function since they are in direct contact with both blood vessels and neurons (Magistretti and Pellerin, 1999; Nedergaard et al., 2003; Sofroniew and Vinters, 2010). To determine whether insulin signaling in astrocytes, in addition to regulating glucose influx into the brain, also directly modifies the responsiveness of hypothalamic neurons to CNS glucose availability, we assessed the feeding responses of mice to direct manipulations of CSF glucose concentrations. Although mice lacking IRs in hypothalamic astrocytes showed less reduction in their food intake following i.c.v. glucose injection, there was no interaction between genotype and the glucose response between groups (Figure 7P). Accordingly, we found that, comparable to what occurred in hypothalamic GFAP-IR WT mice, hypothalamic GFAP-IR KO mice had a normal hyperphagic response when subjected to selective central glucose deprivation by i.c.v. 2DG injection (Figure 7Q). These data indicate that the lack of insulin signaling in astrocytes does not affect glucose responsiveness or the counter-regulatory impact of hypothalamic neurons when glucose fluctuations originate within the BBB. Collectively, our data demonstrate that astrocytic insulin signaling regulates hypothalamic glucose sensing and systemic metabolism via the control of glucose uptake into the brain.

DISCUSSION

Here, we propose a novel model for the functional role of insulin action in the brain. We demonstrated that insulin signaling in

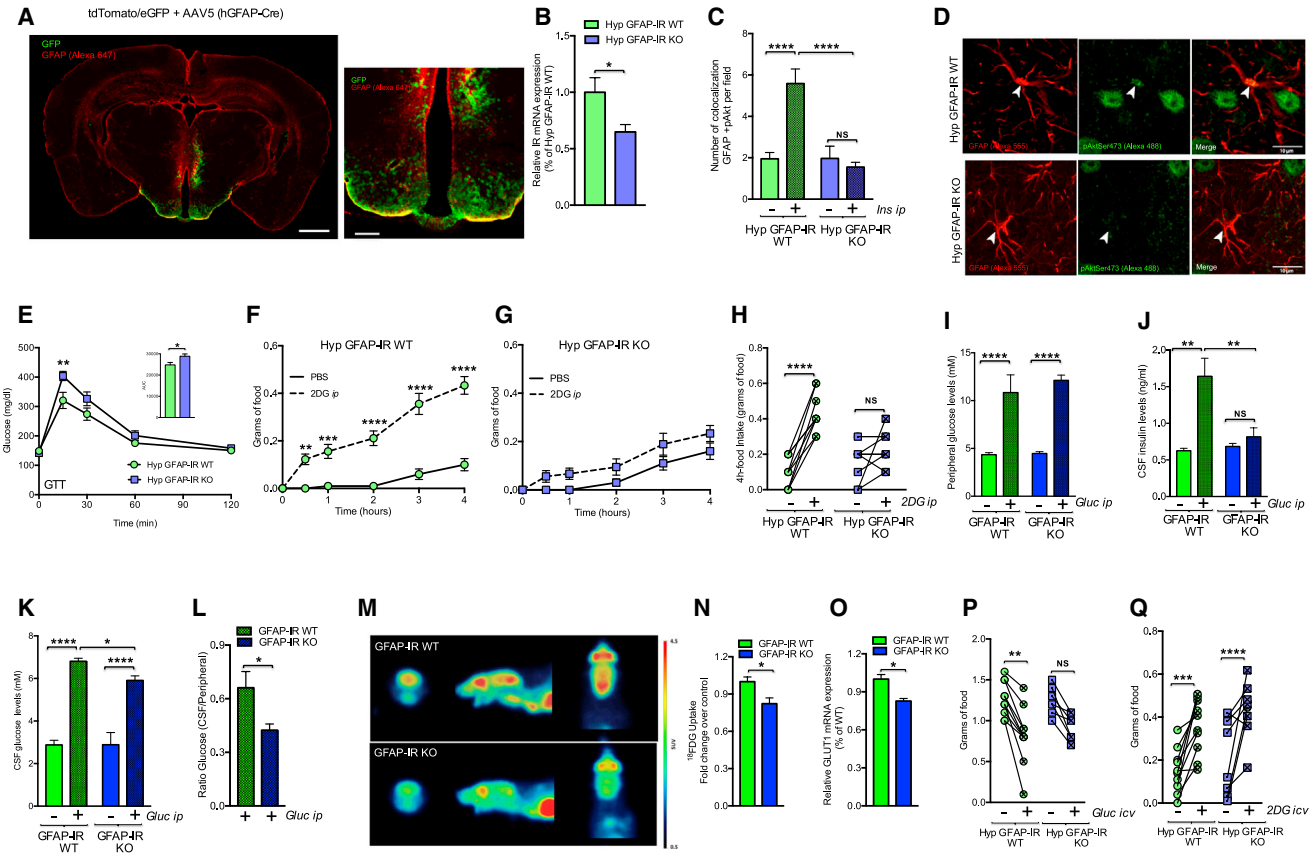

Figure 7. Hypothalamic Insulin Receptors in Astrocytes Regulate Feeding Responses to Adapt to Systemic Glucose Availability and Mediate Proper Glucose and Insulin Entry to the Brain

(A) Mouse brain overview and high magnification depicting the localization of the area infected by AAV5 hGFAP-Cre (GFP-recombined cells under the control of the promoter of hGFAP) and showing GFAP immunoreactivity (red; Alexa 647) in tdTomato/eGFP mice (see also Figure S3N; Table 2).

(B) IR mRNA expression levels corresponding to the hypothalamic region containing virus-targeted astrocytes from C57BL6J mice (n = 6) or $IR^{f/f}$ mice (n = 5) crossed with tdTomato/eGFP mice, which were injected with AAV-hGFAP-Cre in the MBH (see also Figure S3P).

(C) Number of GFAP-positive cells that (co)localize with pAkt in the hypothalamus of $IR^{f/f}$ mice injected with AAV-hGFAP-GFP (Hyp GFAP-IR WT) or AAV-hGFAP-Cre mice (Hyp-GFAP-IR KO) in the MBH 15 min after vehicle (PBS) or insulin injection peripherally (3 U/kg bw; n = 4 mice/group).

(D) Images depicting GFAP-positive cells (red; Alexa 555) and pAkt Ser473 (green; Alexa 488) in the hypothalamus of Hyp GFAP-IR WT mice versus Hyp-GFAP-IR KO mice.

(E) Blood glucose in Hyp GFAP-IR WT mice (n = 9) or Hyp-GFAP-IR KO mice (n = 8) after i.p. glucose.

(F–G) Food intake over the following 4 hr in Hyp GFAP-IR WT (F) or Hyp GFAP-IR KO (G) mice in response to vehicle or i.p. 2DG (n = 9–10/group).

(H) 4 hr accumulated individual changes in food intake after vehicle or i.p. 2DG in Hyp GFAP-IR WT mice and Hyp GFAP-IR KO mice (n = 9–10/group).

(I–L) Glucose content in blood (I), insulin (J) and glucose (K) content in CSF, and the ratio of glucose between CSF versus blood (L) 30 min after i.p. vehicle or glucose in GFAP-IR WT mice versus GFAP-IR KO mice (n = 4–8/group).

(M) ^{18}FDG accumulation in the brain of GFAP-IR WT mice versus GFAP-IR KO mice assessed by positron emission tomography (PET).

(N and O) ^{18}FDG fold change (N) and relative mRNA expression levels of GLUT-1 (O) observed in the brain of GFAP-IR WT mice or GFAP-IR KO mice (n = 4–8/group).

(P and Q) Individual changes of 4 hr food intake after fasting and intracerebroventricular (i.c.v.) injection of vehicle (aCSF) or glucose (1 mg) (P) and individual changes of 4-hr food intake after i.c.v. injection of vehicle (aCSF) or 2-DG (1 mg) (Q) in mice with IR expression in astrocytes in the MBH (Hyp GFAP-IR WT mice; n = 10) or without (Hyp GFAP-IR KO mice; n = 10).

AAV, adeno-associated virus; aCSF, artificial cerebrospinal fluid; GFAP, glial fibrillary acidic protein; GLUT-1, glucose transporter-1; GTT, glucose tolerance test; hGFAP, human glial fibrillary acidic protein; Hyp, hypothalamic; IR, insulin receptor; MBH, the mediobasal hypothalamus; 2DG, 2-deoxy-D-glucose; ^{18}FDG, [^{18}F] fluorodeoxyglucose. ****p < 0.0001; ***p < 0.001; **p < 0.01; *p < 0.05. NS, no significant differences between groups. Data are presented as the mean ± SEM. Scale bars, left panel, 1 mm and right panel, 250 μm (A)and 10 μm (D).

astrocytes is required for efficient glucose uptake into the brain in response to changes in systemic glucose availability. In situations of impaired astroglial insulin signaling, such as in our genetically engineered models or during diet-induced systemic insulin resistance, brain glucose uptake becomes less efficient, thereby compromising hypothalamic glucose sensing and consequently impairing CNS control of systemic glucose homeostasis. For decades, intense efforts have been made to dissect the exact neuronal circuits responsible for glucose sensing in the brain. A potential role for non-neuronal cells, such as astrocytes,

Table 2. Specificity and Efficiency of Inducible Cre-Mediated Recombination in Adult Mice Heterozygous for tdTomato/eGFP Stereotaxically Injected Bilaterally with AAV5-hGFAP-Cre in the Mediobasal Hypothalamus

Specificity (%/Section)	Hypothalamus (%)
% GFAP/GFP	52.2 ± 3.9 (n = 11)
% S100β/GFP	66.2 ± 2.1 (n = 19)
Efficiency (%/Section)	**Hypothalamus (%)**
% GFP/GFAP	59.4 ± 7.0 (n = 8)
% GFP/S100β	53.4 ± 3.8 (n = 16)

however, remained understudied. To uncover a potential role for insulin action on non-neuronal cells in the brain, we used a series of ex vivo and in vivo loss-of-function models to dissect IR function uniquely in astrocytes and to ascertain its relevance for the CNS control of systemic glucose homeostasis. We discovered that insulin signaling in astrocytes plays a key role in allowing efficient hypothalamic neuronal responses in order to appropriately counter fluctuations in systemic glucose availability. Genetic ablation of IRs from GFAP-expressing cells of adult mice altered hypothalamic cellular adaptations corresponding to changes in glucose accessibility in both astrocytes and POMC neurons. In response to elevated blood glucose levels, mice with reduced insulin signaling in GFAP-positive cells had hypothalamic astrocytes with fewer and smaller mitochondria but increased autophagy-related organelles relative to controls. These cellular adaptations are consistent with decreased intracellular glucose availability and lactate release caused by the reduced glucose-uptake capabilities of astrocytes lacking insulin receptors, as we had demonstrated ex vivo. Such metabolic response patterns may seem counterintuitive for astrocytes facing a relative intracellular glucose deficit, but have actually been previously observed, even in situations of glucose depletion (Brown and Ransom, 2007). Beta-oxidation of fatty acids was elevated by the lack of IRs, and was reflected in increased CPT1C expression and elevated etomoxir-sensitive mitochondrial respiration.

Changes in mitochondrial number and architecture were also found in hypothalamic POMC neurons, resulting in an elevated number of disrupted mitochondria and ER-mitochondrial contacts. Recent reports (Dietrich et al., 2013; Schneeberger et al., 2013) have indicated that cells regulate mitochondrial function and architecture as a cellular mechanism of adaptation to energy deficits. This suggests that these glial and neuronal modifications of mitochondrial function might be caused by reduced cellular glucose availability. In addition, we found that mice lacking IRs in astrocytes have altered activity and remodeling of hypothalamic glia and neurons when exposed to high blood glucose levels. This suggests that astrocyte insulin signaling changes in the hypothalamus may modulate morphology and function of the tripartite synapse. Further, a lower activation of POMC neurons was associated with a shift in their synaptic profile.

The CNS constantly responds to hormones and nutrients, including glucose, through a rapid rearrangement of hypothalamic connectivity, evoking the signal transduction necessary for regulating energy homeostasis (Pinto et al., 2004; Zeltser et al., 2012). Therefore, the differences in glial coverage and POMC activity and synaptology that we found might predict alterations in the regulation of feeding behavior and whole-body glucose metabolism that arise as a consequence of deficient astrocytic insulin signaling. Previous studies have indeed reported that changes in the glial distribution around hypothalamic POMC neurons can affect their capacity to respond to variations of glucose (Fuente-Martín et al., 2012).

To corroborate whether IRs in astrocytes are involved in maintaining glucose homeostasis, we examined dynamic responses to altered systemic glucose availability. As expected, mice lacking astrocytic IRs were unable to appropriately curb the normal hyperphagic responses to fasting or glucoprivation. Likewise, exogenous glucose did not suppress hyperphagia and failed to increase c-Fos activity in glucose-sensitive hypothalamic areas. Consistent with this observation, mice lacking astrocytic IRs were also unable to efficiently readjust systemic glucose levels when subjected to hyperglycemia, even when IRs in astrocytes were deleted selectively in the hypothalamus. Similar impairment of systemic glucose metabolism was also found after postnatal ablation of IRs in GLAST-expressing astrocytes. This astrocyte population partially overlaps with GFAP-positive astrocytes and GLAST is almost undetectable in neurons or oligodendrocytes (Mori et al., 2006). This independent set of studies shows that the functional relevance of astrocytic insulin signaling in regulating systemic glucose homeostasis is relevant for more than one population of astrocytes in the brain.

To explore further whether mice failed to curb overfeeding in response to glucose due to insufficient cellular sensing or inefficient uptake of glucose into the brain, we measured brain glucose accumulation in the CSF following peripheral glucose administration. Glucose and insulin availability were both reduced in the CSF in mice lacking astrocytic insulin receptors when subjected to elevated blood glucose levels. Likewise, brain glucose accumulation was also diminished when brain glucose levels where monitored using PET imaging. These observations were paralleled by reduced expression of GLUT-1, the predominant transporter responsible for facilitation of glucose transport across the BBB (Klepper and Voit, 2002).

Cerebral blood vessels are ensheathed by endothelial cells that interact with adjacent astrocytes, the combination regulating the entry of nutrients, such as glucose, by changes in BBB permeability (Alvarez et al., 2013). Although GLUT-1 is highly expressed along the BBB in both endothelial cells and astrocytes (Barros et al., 2007; Simpson et al., 2001), it is more abundant in astrocytes (Simpson et al., 1999). Previous reports indicate that GLUT-1 deficiency leads to restricted delivery of glucose into the brain (Barros et al., 2007; Klepper and Voit, 2002), suggesting that the reduced expression of GLUT-1 observed in the brain of mice without IRs in astrocytes likely decreases glucose transport across the BBB, resulting in lower CSF glucose concentrations. Recently, alterations in GLUT-1 expression at the BBB were associated with the development of neurodegenerative diseases, including Alzheimer's disease (AD). In fact, early reductions in GLUT-1 at the BBB have been implicated in the pathogenesis of AD, promoting neuro-vascular dysfunction associated with AD progression (Winkler et al., 2015). Indeed, a link between AD and insulin resistance is

currently emerging in a model whereby insulin signaling deficiencies contribute to develop the neuropathy and cognitive decline associated with the development of AD (De Felice and Ferreira, 2014; Ferreira et al., 2014). Therefore, insulin signaling/GLUT-1 interventions in astrocytes might represent useful therapeutic targets to prevent or slow down neurodegeneration and cognitive defects associated with the progression of AD. Finally, we have found that insulin signaling in astrocytes is expendable for central glucose responsiveness when glucose fluctuations originate inside the BBB. Central manipulations of glucose reversed the phenotype of mice lacking astrocytic IR. That said, it is unknown if the long-lasting effects of a glucose-transport deficiency into the brain might increase the risk to elicit alterations in glucose sensitivity. Collectively, our findings indicate that insulin signaling in astrocytes is required to interlink CNS glucose levels with systemic nutrient availability and is therefore indispensable for an appropriate regulation of systemic glucose homeostasis.

Conclusions

Here, we have demonstrated that insulin signaling in astrocytes co-regulates behavioral responses and metabolic processes via control of brain glucose uptake to maintain systemic glucose homeostasis. Specifically, our findings uncover a role for insulin action in non-neuronal cells of the hypothalamus to regulate glucose entry into the CNS. Consistent with a model whereby astrocytes are functionally involved in both nutrient sensing and the CNS control of systemic metabolism, we have recently reported that astrocytes respond to another afferent metabolic hormone, leptin. Astrocytic leptin deficiency also affects glial structure, ensheathment of hypothalamic POMC neurons, and feeding responses (Kim et al., 2014). We therefore propose a model whereby, similar to neurons, astrocytes respond directly to a plethora of nutrient and endocrine signals and, in turn, contribute to adjusting CNS control of systemic metabolism according to nutrient availability. This model may offer improved strategies for the discovery of novel therapeutics for metabolic and neurodegenerative diseases.

EXPERIMENTAL PROCEDURES

Animals

hGFAP-CreER^{T2} are Tx-inducible transgenic mice in which the Cre transgene is expressed under the control of the hGFAP promotor. These mice were generated on a C57BL/6J background (provided by F.M. Vaccarino, Yale University School of Medicine) and were mated with mice having the sequence of the IR gene flanked by loxP sites (IR$^{f/f}$) (generated by Ronald Kahn, Joslin Diabetes Center). Mouse cohorts for experiments were generated by mating IR$^{f/f}$ and hGFAP-CreER^{T2}:IR$^{f/f}$ mice.

In parallel, GLAST ^{CreERT2}, a knockin mouse line, was obtained and crossed with IR$^{f/f}$ mice. In this model, the Cre^{ERT2} allele is expressed in the locus of the control of the astrocyte-specific glutamate-aspartate transporter (GLAST) locus (Mori et al., 2006). Mice were generated by mating GLAST^{CreERT2} mice and GLAST^{CreERT2}: IR$^{f/f}$ mice. All experiments with GLAST-specific KO mouse models were performed with the GLAST^{CreERT2} allele in heterozygotes.

To evaluate whether astrocytic mitochondrial or energy signals deregulation causes systemic glucose metabolic alterations, we crossed hGFAP-CreER^{T2} mice with UCP2$^{f/f}$ mice (Jackson Laboratory, stock no. 022394) or double combination of IR$^{f/f}$ mice and LepR$^{f/f}$ mice (McMinn et al., 2005). Cohorts of mice were generated by mating UCP2$^{f/f}$ mice and hGFAP-CreER^{T2}:UCP2$^{f/f}$ mice or IR$^{f/f}$:LepR$^{f/f}$ mice and hGFAP-CreER^{T2}:IR$^{f/f}$:LepRf/f mice, respectively.

To excise loxP sites by Cre recombination (see also the Supplemental Experimental Procedures), 6-week-old male mice were injected daily with Tx (10 mg per kg of body weight, i.p.) for 5 days. Tx (Sigma) was dissolved in sunflower oil at a final concentration of 10 mg/ml at 37°C and then filter sterilized and stored for up to 7 days at 4°C in the dark.

All mice were housed on a 12:12-hr light-dark cycle at 22°C with free access to food and water, unless indicated otherwise. They were maintained on a pelleted chow diet (5.6% fat; LM-485, Harlan Teklad) until 12 weeks of age. Subsequently, the mice were either maintained on chow or switched to high-fat, high-sugar (HFHS: 58% kcal fat w/sucrose; Research Diets) diet for 12 weeks. All studies were approved by and performed in accordance with the guidelines of the Institutional Animal Care and Use Committee of Cajal Institute, Yale University, and the Helmholtz Centre Munich.

Glucose Tolerance Test, Insulin Tolerance Test, and Insulin Secretion Test

Mice were subjected to 6 hr of fasting and then injected i.p. with glucose (2 g/kg body weight of D-glucose in 0.9% saline) for the glucose tolerance test (GTT) and 0.75 U/kg bw of insulin (0.1 U/ml; Humolog Pen, Eli Lilly) for the insulin tolerance test (ITT). Tail-blood glucose levels (mg/dl) were measured with a handheld glucometer (TheraSense Freestyle) at the following time points: 0, 15, 30, 60, and 120 min after injection. For the insulin secretion test (IST), blood samples were collected at 0, 15, and 30 min after glucose injection (2 g of glucose /kg body weight) for insulin determination by ELISA.

Feeding Experiments

For all feeding experiments, mice (3 months of age) were individually housed and fed a chow diet (see also the Supplemental Experimental Procedures).

Astrocyte-Specific Cre-Mediated Recombination by Adeno-Associated Virus Bilaterally Injected into the MBH

In order to ablate IRs specifically in astrocytes, we used adeno-associated virus (AAV) viral particles (serotype 2/5) expressing GFP or Cre protein under control of the hGFAP promoter (Vector Biolabs). We stereotaxically injected AAV-hGFAP-GFP (hypothalamic GFAP-IR WT) or AAV-hGFAP-Cre (hypothalamic GFAP-IR KO) particles bilaterally (2×10^9 viral genome particles per side) into the MBH of IR$^{f/f}$ littermates by using a motorized stereotaxic device (Neurostar). Stereotaxic coordinates were −1.5 mm posterior and −0.3 mm lateral to bregma, and −5.8 mm ventral from the dura. Surgeries were performed using a mixture of ketamine and xylazine (100 and 7 mg/kg, respectively) as anesthetic agents and Metamizol (50 mg/kg, subcutaneous [s.c.]) followed by Meloxicam (1 mg/kg, on 3 consecutive days s.c.) for postoperative analgesia.

Primary Astrocyte Cultures Collection and Adenovirus-Cre In Vitro Infection Mediated IR Knockout

Hypothalami and cortices were extracted from IR$^{f/f}$ male mice at postnatal day 1 and were dissociated to single cells as previously described (Fuente-Martín et al., 2012).

Hypothalamic or cortical astrocyte cultures were seeded onto 6-well plates in DMEM-F12 supplemented with 10% fetal bovine serum (FBS) and antibiotic (penicillin 100 IU/ml and streptomycin 100 micro-g/ml) in 5% CO_2 at 37°C. After 24 hr, cells were incubated with Adenovirus-GFP (AAV(5)-GFAP(2.2)-GFP, 1×10^{13} gc/ml; WT) or Adenovirus-Cre-mediated deletion of allele with loxP sites coexpressed with GFP (AAV(5)-GFAP(2.2)-iCre, $1x\ 10^{13}$ gc/ml; KO) from Baylor College of Medicine in DMEM-F12 supplemented with 1% FBS for 6 hr in 5% CO_2 at 37°C. To increase the binding of adenovirus to the cell surface, we added 0.25% of AdenoBOOST (Sirion Biotech). After extensive washing in PBS, cells were incubated in DMEM-F12 with 10% FBS for 3 days.

Statistical Analyses

All statistical analyses were performed using GraphPad Prism. Two groups were compared by using two-tailed unpaired Student's t test. Two-way ANOVA was performed to detect significant interactions between genotype and treatment (tamoxifen, glucose, insulin, or 2DG), and multiple comparisons

were analyzed following Bonferroni's post hoc tests. Two-way repeated measures ANOVA was performed to detect significant interactions between genotype and time, and multiple comparisons were analyzed following Bonferroni's post hoc tests. p values lower than 0.05 were considered significant. All results are presented as means ± SEM.

SUPPLEMENTAL INFORMATION

Supplemental Information includes Supplemental Experimental Procedures and three figures and can be found with this article online at http://dx.doi.org/10.1016/j.cell.2016.07.028.

AUTHOR CONTRIBUTIONS

C.G.-C. and M.H.T. conceptualized all studies and designed all experiments. C.G.-C., C.Q., L.V., Y.G., T.G., B.L., P.J., O.L.T., K.S.-B., W.C., A.M.F., and I.T.-A. performed the experiments and collected the data. C.G.-C., C.Q., and L.V. analyzed the data. M.H.T., T.L.H., and C.G.-C. wrote the manuscript in discussion with M.J., C.W.M., P.T.P., S.C.W., J.N., S.L., C.R.K., and M.G., who critically revised the article for important intellectual content. All authors have read and approved the final version of the manuscript.

ACKNOWLEDGMENTS

The authors thank Heicko Lickert and Silke Morin for helpful discussion and support and Lewis Norris, Clarita Mergen, Veronica Casquero García, Olavi Järvinen, and Nicole Wiegert for excellent technical assistance. This work was funded, in part, by the Helmholtz Alliance ICEMED – Imaging and Curing Environmental Metabolic Diseases, the Humboldt Foundation (to M.H.T.), through the Initiative and Networking Fund of the Helmholtz Association and Deutsches Zentrum für DiabetesForschung (DZD). This work also received funding from the Institute of Advanced Studies of Technische Universität München (IAS-TUM Hans-Fischer Senior Fellowship to T.L.H.) and from DFG funding (SFB 1123 to M.H.T; SFB 870 and SPP 1757 to M.G.).

Received: October 29, 2015
Revised: May 31, 2016
Accepted: July 19, 2016
Published: August 11, 2016

REFERENCES

Abbott, N.J., Rönnbäck, L., and Hansson, E. (2006). Astrocyte-endothelial interactions at the blood-brain barrier. Nat. Rev. Neurosci. *7*, 41–53.

Alvarez, J.I., Katayama, T., and Prat, A. (2013). Glial influence on the blood brain barrier. Glia *61*, 1939–1958.

Armulik, A., Genové, G., Mäe, M., Nisancioglu, M.H., Wallgard, E., Niaudet, C., He, L., Norlin, J., Lindblom, P., Strittmatter, K., et al. (2010). Pericytes regulate the blood-brain barrier. Nature *468*, 557–561.

Baltzer, C., Tiefenböck, S.K., and Frei, C. (2010). Mitochondria in response to nutrients and nutrient-sensitive pathways. Mitochondrion *10*, 589–597.

Barros, L.F., Bittner, C.X., Loaiza, A., and Porras, O.H. (2007). A quantitative overview of glucose dynamics in the gliovascular unit. Glia *55*, 1222–1237.

Brown, A.M., and Ransom, B.R. (2007). Astrocyte glycogen and brain energy metabolism. Glia *55*, 1263–1271.

Brüning, J.C., Gautam, D., Burks, D.J., Gillette, J., Schubert, M., Orban, P.C., Klein, R., Krone, W., Müller-Wieland, D., and Kahn, C.R. (2000). Role of brain insulin receptor in control of body weight and reproduction. Science *289*, 2122–2125.

Buffo, A., Rite, I., Tripathi, P., Lepier, A., Colak, D., Horn, A.P., Mori, T., and Götz, M. (2008). Origin and progeny of reactive gliosis: A source of multipotent cells in the injured brain. Proc. Natl. Acad. Sci. USA *105*, 3581–3586.

Cranston, I., Marsden, P., Matyka, K., Evans, M., Lomas, J., Sonksen, P., Maisey, M., and Amiel, S.A. (1998). Regional differences in cerebral blood flow and glucose utilization in diabetic man: the effect of insulin. J. Cereb. Blood Flow Metab. *18*, 130–140.

De Felice, F.G., and Ferreira, S.T. (2014). Inflammation, defective insulin signaling, and mitochondrial dysfunction as common molecular denominators connecting type 2 diabetes to Alzheimer disease. Diabetes *63*, 2262–2272.

Dietrich, M.O., Liu, Z.W., and Horvath, T.L. (2013). Mitochondrial dynamics controlled by mitofusins regulate Agrp neuronal activity and diet-induced obesity. Cell *155*, 188–199.

Ferreira, S.T., Clarke, J.R., Bomfim, T.R., and De Felice, F.G. (2014). Inflammation, defective insulin signaling, and neuronal dysfunction in Alzheimer's disease. Alzheimers Dement. *10* (1, Suppl), S76–S83.

Frank, H.J., Pardridge, W.M., Morris, W.L., Rosenfeld, R.G., and Choi, T.B. (1986). Binding and internalization of insulin and insulin-like growth factors by isolated brain microvessels. Diabetes *35*, 654–661.

Fuente-Martín, E., García-Cáceres, C., Granado, M., de Ceballos, M.L., Sánchez-Garrido, M.A., Sarman, B., Liu, Z.W., Dietrich, M.O., Tena-Sempere, M., Argente-Arizón, P., et al. (2012). Leptin regulates glutamate and glucose transporters in hypothalamic astrocytes. J. Clin. Invest. *122*, 3900–3913.

Ganat, Y.M., Silbereis, J., Cave, C., Ngu, H., Anderson, G.M., Ohkubo, Y., Ment, L.R., and Vaccarino, F.M. (2006). Early postnatal astroglial cells produce multilineage precursors and neural stem cells in vivo. J. Neurosci. *26*, 8609–8621.

García-Cáceres, C., Fuente-Martín, E., Argente, J., and Chowen, J.A. (2012). Emerging role of glial cells in the control of body weight. Mol. Metab. *1*, 37–46.

Goldman, S. (2003). Glia as neural progenitor cells. Trends Neurosci. *26*, 590–596.

Hasselbalch, S.G., Knudsen, G.M., Videbaek, C., Pinborg, L.H., Schmidt, J.F., Holm, S., and Paulson, O.B. (1999). No effect of insulin on glucose blood-brain barrier transport and cerebral metabolism in humans. Diabetes *48*, 1915–1921.

Havrankova, J., Roth, J., and Brownstein, M. (1978). Insulin receptors are widely distributed in the central nervous system of the rat. Nature *272*, 827–829.

Kim, J.G., Suyama, S., Koch, M., Jin, S., Argente-Arizon, P., Argente, J., Liu, Z.W., Zimmer, M.R., Jeong, J.K., Szigeti-Buck, K., et al. (2014). Leptin signaling in astrocytes regulates hypothalamic neuronal circuits and feeding. Nat. Neurosci. *17*, 908–910.

Kleinridders, A., Ferris, H.A., Cai, W., and Kahn, C.R. (2014). Insulin action in brain regulates systemic metabolism and brain function. Diabetes *63*, 2232–2243.

Klepper, J., and Voit, T. (2002). Facilitated glucose transporter protein type 1 (GLUT1) deficiency syndrome: impaired glucose transport into brain– a review. Eur. J. Pediatr. *161*, 295–304.

Koch, L., Wunderlich, F.T., Seibler, J., Könner, A.C., Hampel, B., Irlenbusch, S., Brabant, G., Kahn, C.R., Schwenk, F., and Brüning, J.C. (2008). Central insulin action regulates peripheral glucose and fat metabolism in mice. J. Clin. Invest. *118*, 2132–2147.

Magistretti, P.J., and Pellerin, L. (1999). Cellular mechanisms of brain energy metabolism and their relevance to functional brain imaging. Philos. Trans. R. Soc. Lond. B Biol. Sci. *354*, 1155–1163.

Mandl, J., Mészáros, T., Bánhegyi, G., Hunyady, L., and Csala, M. (2009). Endoplasmic reticulum: nutrient sensor in physiology and pathology. Trends Endocrinol. Metab. *20*, 194–201.

McMinn, J.E., Liu, S.M., Liu, H., Dragatsis, I., Dietrich, P., Ludwig, T., Boozer, C.N., and Chua, S.C., Jr. (2005). Neuronal deletion of Lepr elicits diabesity in mice without affecting cold tolerance or fertility. Am. J. Physiol. Endocrinol. Metab. *289*, E403–E411.

Mori, T., Tanaka, K., Buffo, A., Wurst, W., Kühn, R., and Götz, M. (2006). Inducible gene deletion in astroglia and radial glia–a valuable tool for functional and lineage analysis. Glia *54*, 21–34.

Nedergaard, M., Ransom, B., and Goldman, S.A. (2003). New roles for astrocytes: redefining the functional architecture of the brain. Trends Neurosci. *26*, 523–530.

Nolte, C., Matyash, M., Pivneva, T., Schipke, C.G., Ohlemeyer, C., Hanisch, U.K., Kirchhoff, F., and Kettenmann, H. (2001). GFAP promoter-controlled EGFP-expressing transgenic mice: a tool to visualize astrocytes and astrogliosis in living brain tissue. Glia *33*, 72–86.

Pinto, S., Roseberry, A.G., Liu, H., Diano, S., Shanabrough, M., Cai, X., Friedman, J.M., and Horvath, T.L. (2004). Rapid rewiring of arcuate nucleus feeding circuits by leptin. Science *304*, 110–115.

Schneeberger, M., Dietrich, M.O., Sebastián, D., Imbernón, M., Castaño, C., Garcia, A., Esteban, Y., Gonzalez-Franquesa, A., Rodríguez, I.C., Bortolozzi, A., et al. (2013). Mitofusin 2 in POMC neurons connects ER stress with leptin resistance and energy imbalance. Cell *155*, 172–187.

Simpson, I.A., Appel, N.M., Hokari, M., Oki, J., Holman, G.D., Maher, F., Koehler-Stec, E.M., Vannucci, S.J., and Smith, Q.R. (1999). Blood-brain barrier glucose transporter: effects of hypo- and hyperglycemia revisited. J. Neurochem. *72*, 238–247.

Simpson, I.A., Vannucci, S.J., DeJoseph, M.R., and Hawkins, R.A. (2001). Glucose transporter asymmetries in the bovine blood-brain barrier. J. Biol. Chem. *276*, 12725–12729.

Smith, G.P., and Epstein, A.N. (1969). Increased feeding in response to decreased glucose utilization in the rat and monkey. Am. J. Physiol. *217*, 1083–1087.

Sofroniew, M.V., and Vinters, H.V. (2010). Astrocytes: biology and pathology. Acta Neuropathol. *119*, 7–35.

Toran-Allerand, C.D., Bentham, W., Miranda, R.C., and Anderson, J.P. (1991). Insulin influences astroglial morphology and glial fibrillary acidic protein (GFAP) expression in organotypic cultures. Brain Res. *558*, 296–304.

Tubbs, E., Theurey, P., Vial, G., Bendridi, N., Bravard, A., Chauvin, M.A., Ji-Cao, J., Zoulim, F., Bartosch, B., Ovize, M., et al. (2014). Mitochondria-associated endoplasmic reticulum membrane (MAM) integrity is required for insulin signaling and is implicated in hepatic insulin resistance. Diabetes *63*, 3279–3294.

Winkler, E.A., Nishida, Y., Sagare, A.P., Rege, S.V., Bell, R.D., Perlmutter, D., Sengillo, J.D., Hillman, S., Kong, P., Nelson, A.R., et al. (2015). GLUT1 reductions exacerbate Alzheimer's disease vasculo-neuronal dysfunction and degeneration. Nat. Neurosci. *18*, 521–530.

Woods, S.C., Lotter, E.C., McKay, L.D., and Porte, D., Jr. (1979). Chronic intracerebroventricular infusion of insulin reduces food intake and body weight of baboons. Nature *282*, 503–505.

Zeltser, L.M., Seeley, R.J., and Tschöp, M.H. (2012). Synaptic plasticity in neuronal circuits regulating energy balance. Nat. Neurosci. *15*, 1336–1342.